Hindawi
Shock and Vibration
Volume 2023, Article ID 1565927, 11 pages
https://doi.org/10.1155/2023/1565927

Research Article

Effect of Ultrasonic Vibration on Forming Force in the Single-Point Incremental Forming Process

Trung-Kien Le,[1] **Duc-Toan Tran**,[2,3] **Ngoc-Tam Bui Bui**,[4] **and Thanh-Hai Nguyen**[2,3]

[1]*School of Mechanical Engineering, Hanoi University of Science and Technology, Hanoi 10000, Vietnam*
[2]*Faculty of Mechanical Engineering, Ho Chi Minh City University of Technology (HCMUT), Ho Chi Minh 700000, Vietnam*
[3]*Viet Nam National University of Ho Chi Minh City (VNUHCM), Linh Trung Ward, Thu Duc District, Ho Chi Minh 700000, Vietnam*
[4]*College of Systems Engineering and Science, Shibaura Institute of Technology, Tokyo 135-8548, Japan*

Correspondence should be addressed to Thanh-Hai Nguyen; haint@hcmut.edu.vn

Received 7 September 2022; Revised 20 February 2023; Accepted 29 March 2023; Published 17 April 2023

Academic Editor: Francisco Beltran-Carbajal

Single-point incremental forming (SPIF) has drawn much attention recently due to its flexibility in making parts for rapid prototypes and small samples. Several studies have pointed out the benefits of using ultrasonic vibration (UV) in SPIF experimentally. This study verifies the effect of UV in reducing the forming forces by performing numerical simulations. In addition, the effect of several process parameters, including tool diameters, rotational speeds, step sizes, and ultrasonic vibration amplitudes, is investigated in detail. It is found that an increase in the tool rotational speed and vibrating amplitude decreases forming forces, whereas an increase in the vertical step size increases forming forces.

1. Introduction

Ultrasonic vibration (UV) is added in many machining and deformation processes such as drilling [1], turning [2, 3], and forging [4, 5]. Drilling force decreases when UV is applied. Surface roughness is reduced by adding UV in microforging [6]. In the turning process with UV-assisted [7], forming force declines by 40% to 45% and temperature drops by 48%. Similarly, cutting force, surface quality, and tool wear are improved [8]. In UV-assisted grinding [9], normal and tangential grinding force decreases by 60% and 40%, respectively. Moreover, under the effect of UV, the extrusion force decreased by an increase in the temperature of workpiece [10].

Incremental sheet forming (ISF) has been applied widely for producing sheet products. ISF brings benefits compared with the conventional process and the ability of rapid prototyping and producing complex parts in a small volume without the use of expensive equipment. However, ISF has drawbacks, such as long manufacturing time, poor dimensions, low surface quality, and difficulty to form high strength materials.

Zhan et al. [11] studied the SPIF process for AA2024-T3 under high-speed tool rotation. The evolution of damage and prediction of the fracture forming limits of SPIF processes is investigated numerically.

Martin [12] studied rapid prototyping by single-point incremental forming of sheet metal. The study proposed a new theory to explain the high formability of the process. A thin membrane equation was developed to calculate stress in the deformed area to prove that fracture in the SPIF process was less than other regular sheet-forming processes.

João Luís Padrão Câmara [13] continued to study the deformation mechanism of the aluminum sheet during conventional and multistage SPIF processes. The research also proved that necking stage occurred in parts that were manufactured with the bigger tool. The multistage SPIF process could enhance formability, and the results confirmed that the SPIF process was limited by fracture and not by necking.

Other noticeable studies on the SPIF process [14] focused on the conventional spinning and SPIF processes. In the SPIF process, the main factors were normal and tangential shear, stretching, thinning, and bending. Other parameters that affected the part quality were tool diameter, step size, sheet thickness, and friction. The geometry errors such as bending, spring back, and pillow effect at the center of the sheet were reduced by using the backing plate, kinematic supporting tool, and tool path modification.

A study of the deformation mechanism in the SPIF process was conducted [15]. It shows that high formability and manufactured depth can be achieved with a wall angle less than 75°. When the wall angle decreased, deformation occurred mainly due to shear stress. By increasing the wall angle, tensile stress had a more critical impact than shear stress.

The formability of the SPIF process was improved by using electrical current, contact area prediction, and tool development. Electrical current can increase the formability in 6061-T6 aluminum and stainless steel 304. Abnormal shape tools such as parabolic shape can obtain better formability and surface quality [16].

In 1955, Langnecker had investigated the effect of ultrasonic vibration (UV) on the material [17], and the results showed that there is a reduction in flow stress and that the softening in the material makes it easier for forming. Since then, many studies have been conducted on ISF with ultrasonic vibrating tools [18].

Li et al. have studied on how the formability of ISF changes when applying UV. Ultrasonic vibration had a remarkable influence during the ISF process with a high reduction in forming forces, especially at larger stages, and the softening effect was proportional to the vibration amplitude. The authors also investigated the reduction of forming forces when changing different parameters [19, 20].

The material flow and deformation behaviour during UV-a-SPIF of making straight grooves was studied. After applying UV, the material flow area significantly increased and was proportional to the ultrasonic vibration amplitude. The adoption of UV also increased the grain size and decreased the misorientation angle of the formed parts [21].

The forming forces between SPIF and UV-a-SPIF were compared [22]. The force reduction in the axial force (F_z) and planar force (F_x) was 23.5% and 26.3%, respectively. The results also showed higher formable depth, lower springback coefficient, and considerably lower surface roughness value under the effect of UV.

A study on the effect of UV both single-point and two-point incremental forming [23] was conducted. Applying UV in ISF significantly reduced forming forces. In TPIF, the force values were lower than SPIF and the reduction value increased as the vibration amplitude increased. However, the force reduction is significantly lower than results from [22], at 4.7% to 18% reduction compared to 23.5% and 26.3%.

The effect of rotational speed and UV on forming forces, surface roughness, hardness, and tensile limit in ISF was studied [24]. The increased rotational speed decreased informing forces due to the reduction in friction and the local heat generated between the tool and the sheet. Besides, implementing both rotating tools and ultrasonic vibration in ISF can increase the stretching limit up to 41.79%.

The distribution of sheet thickness during the process of UV-a-SPIF was focused [25]. The thinnest and most vulnerable to the fracture area was the center of the sidewall of the pyramid, and the thinning rate was symmetrically distributed from the center of the sidewall to the bottom and the top. Additionally, the vibration frequency had a significant impact on the forming angle. A frequency higher than 25 kHz can decrease the forming angle, whereas a frequency from 0 to 25 kHz increased formability.

The SPIF process with UV and static pressure support (SPS) improved the product accuracy. Axial and planar forces were related to static pressure, amplitude, frequency, tool diameter, step size, sheet thickness, and feed rate. The effect of SPS and UV was nonlinear [26].

High formability of UV-a-SPIF came from the acoustoplasticity phenomenon, also known as the "Blaha effect." Acoustoplasticity created a softening effect in the material, resulting in flow stress reduction, when UV was imposed into the process. Besides, flow stress reduction, other advantages such as reduction in friction, better surface finish and higher geometric accuracy, enhanced material properties, and refined microstructures also had been reported [27, 28].

This study focuses on the simulation of the SPIF process using the ultrasonic vibrating tool by ABAQUS. Two types of simulation were also carried out: straight groove and truncated pyramid. The process parameters of tool diameter, rotational speed, step size, and vibration amplitude were investigated. The forming force is reduced in the UV-a-SPIF process.

2. Materials and Methods

2.1. Ultrasonic Vibration Assisted in Single-Point Incremental Forming. In SPIF, the part is localized deformed by moving a tool over the workpiece. The localized deformation strategy is the main advantage that makes the formability of ISF higher than that of the conventional process. A tool is a hemispherical-head tool with a diameter commonly ranging from 5 to 20 mm. The forming tool is numerically controlled by using a CNC machine or robotic arms with the tool path programmed based on the part profile and generated by the CAD/CAM program. To create the part, the tool first plunges into the workpiece and then follows the periphery of the part. The tool continues to move to the next layer, and the process repeats until the tool reaches the desired depth of the part. In UV-a-SPIF, the tool is connected to an ultrasonic system, which makes the tool vibration in the vertical direction, as shown in Figure 1.

2.2. Simulation of UV-a-SPIF. In this study, two finite element (FE) models were developed in ABAQUS/explicit software to simulate the two UV-a-SPIF processes: straight groove and a truncated pyramid. The investigated material is AA5052-H32 sheet with a thickness of 1.0 mm. Material properties including the Young modulus, Poisson ratio, and

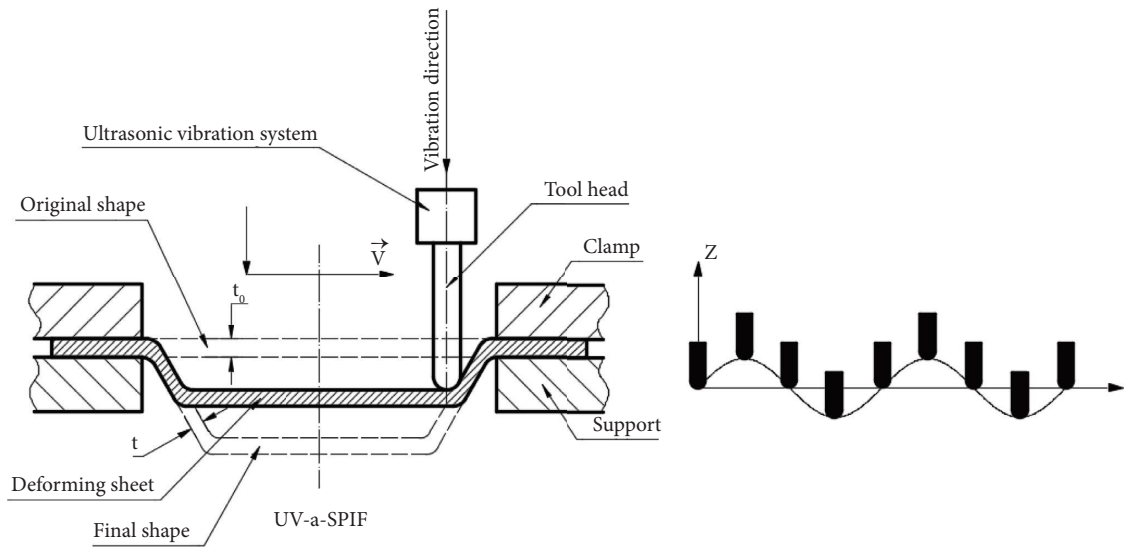

Figure 1: Schematic of the UV-a-SPIF process with sinusoidal horizontal movement of the tool.

stress-strain curve were adopted from the data reported in [29].

In the simulation of a straight groove, a blank sheet with a size of 150 × 90 mm is modelled. Deformation is concentrated in the center of the sheet, with a length of 60 mm, as shown in Figure 2. Therefore, a deformed area of 60 × 10 mm is modelled with fine meshes, whereas the rest area is meshed with larger elements. A hemispherical rigid tool with a diameter of 10 mm is used to deform the sheet. The supporting die is also assigned as discrete rigid to prevent deformation during the process. The details of the developed FE model are presented in Figure 3.

Following the mesh size and mesh type analysis [27], in this model, four-node shell elements with reduced integration are used to model the sheet with a mesh size of 0.5 mm in the center region. The edges of the blank fix all degrees of freedom before the forming process. During the test, the tool is moved following the tool path described in Figure 4(a) to deform the sheet. To assign tool vibration in the vertical direction, a periodic amplitude function in ABAQUS is called. A frequency of 20 kHz is targeted to the vibration. However, using a physical time in simulations of SPIF leads to unacceptable actual running time. Therefore, a virtual step time of 0.01 s is assigned for each step. As a result, the imposed frequency of vibration is scaled according to the virtual step time. According to [12], the friction coefficient is around 0.05 to 0.5; we take into account of 0.3 as the friction coefficient for the simulation. For the simplicity of the simulation, this study excludes heat generated during the process.

A similar model is developed to simulate the UV-a-SPIF of a truncated pyramid. The dimension of the sheet used in this simulation is of 140 × 140 mm, whereas a center region of 40 × 40 mm is modelled with smaller elements, as shown in Figure 5. It is worth noticing that the tool path used to form the pyramid is illustrated in Figure 4.

3. Results and Discussion

3.1. Simulation of Straight Grooves. Figure 6 shows the deformed shape obtained from the simulation of making a straight groove. Table 1 reports the simulated forces according to the models with and without UV.

In Table 1, it is clear that the forming force is reduced under UV effects. However, the reduction in force values is relatively small; the different value is 6 N (approximately 0.7%). The average force of F_x is significantly lower than that of F_z; this means that the total force value is heavily dependent on F_z.

In Figures 7 and 8, the planar and axial forces increase as the tool plunges into the part deeper. This force fluctuation caused by the direction of vibration along the vertical axis which the tool constantly makes contact with and lifts off the surface of the workpiece. As a result, the force rises up as the tool presses onto the sheet and declines when the tool goes up. Both forces from UV simulations oscillate greater than in regular SPIF simulations, whereas during regular SPIF, the tool remains in contact with the workpiece; therefore, the force stays persistent.

At the end of each plunging step in the simulation, the forming force rapidly increases, reaching the maximum value at 2169.9 N, which is much higher than the forming forces during the main pathing stages.

3.2. Simulation of the Truncated Pyramid. The stress distribution, Figure 9, in the final part is not uniform. The stress value in the corner seemed to be lower than the sidewall. The area with a higher stress value is located from the center of the sidewall to the curve side in the bottom of the part, while the upper part has a lower stress value. It can be explained by the difference of the fillet radius. The bottom fillet radius is 5 mm caused by the tool, whereas the fillet radius on the top is significantly bigger.

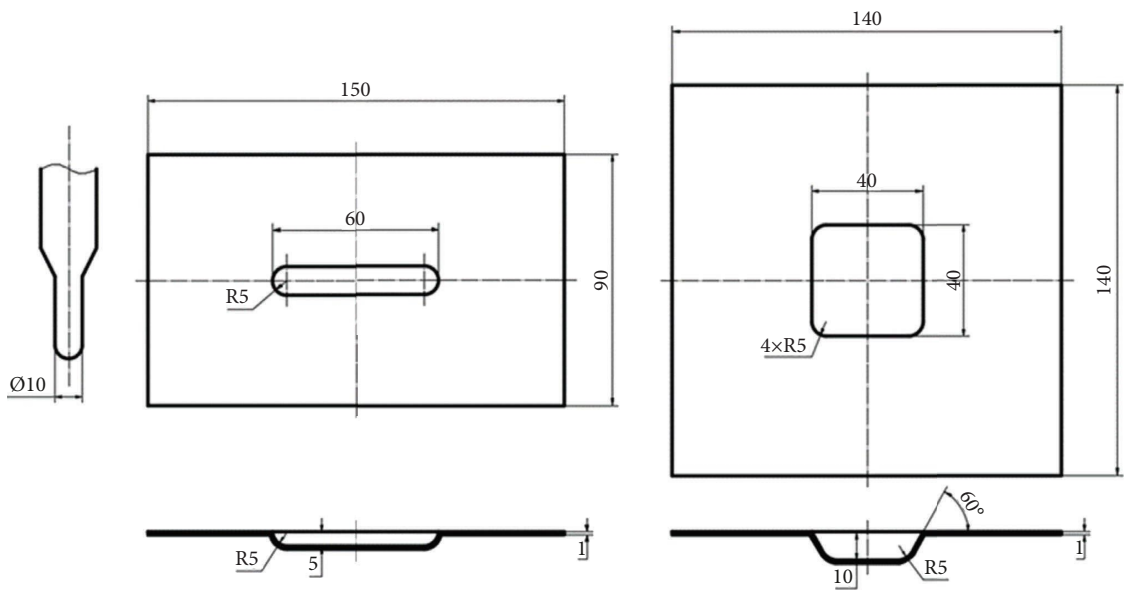

Figure 2: Dimension of tools and part in the simulations.

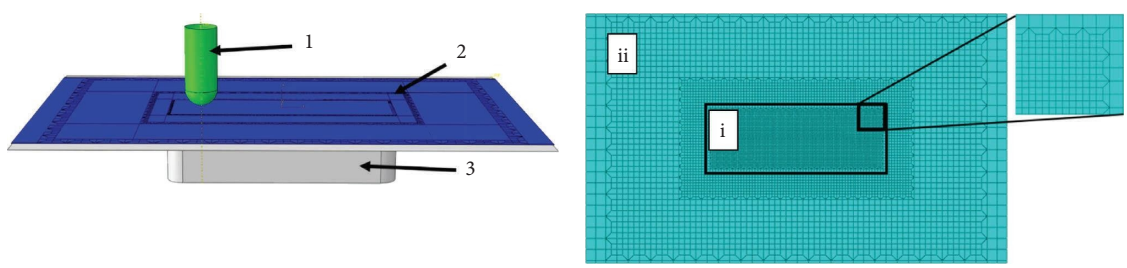

(a) (b)

Figure 3: Setup of the simulation of a straight groove: (a) FE model with (1) tool head, (2) metal sheet, and (3) supporting die; (b) Mesh on the sheet with a (area i) fined mesh area and (area ii) large mesh area.

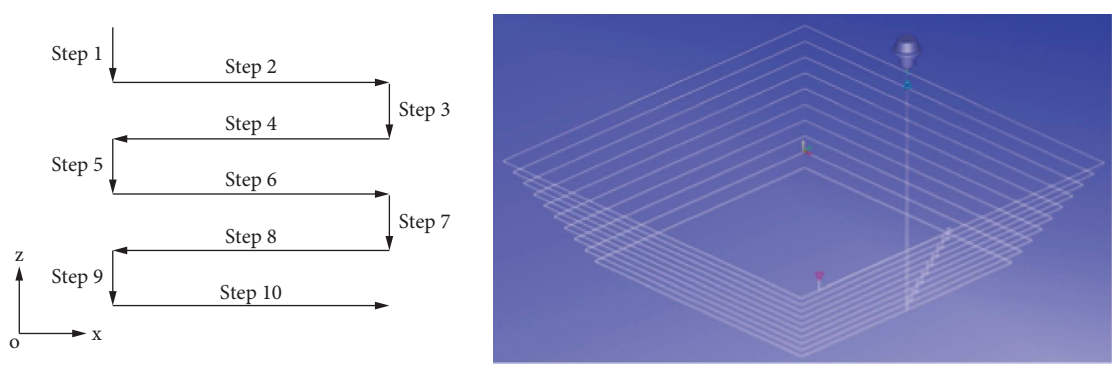

Figure 4: Tool path used in the straight groove and truncated pyramid tests.

Compared to the simulation in straight grooves, the results in this test (as shown in Figure 10 and Table 2) indicate a shift in the direction of Fx and Fy, resulting in a lower average value. Consequently, the total forming force is determined by the average value of F_z. As expected, by applying UV in SPIF, the forming force and component forces are reduced, even though the reduction is relatively small. The forming force difference is at 13.3 N, approximately 1.7%, which is higher than that in the straight groove tests. The forming force with UV fluctuates greater than without UV due to the vertical vibration of the tool. Despite the significant fluctuation in force, the F_z graph from UV simulations still lies beneath the F graph from non-UV simulations. Besides, the forming force increases gradually in the early stages and then tends to remain consistent during later forming stages.

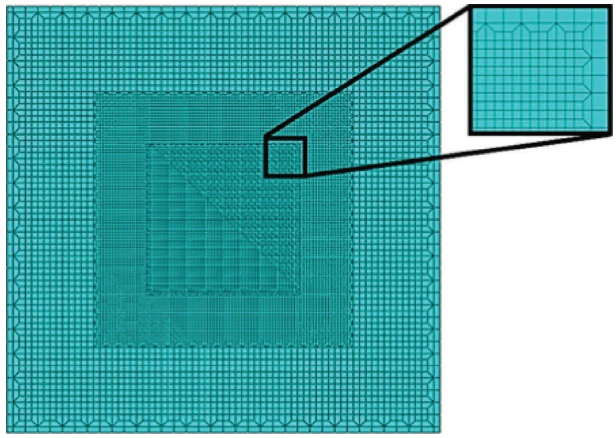

Figure 5: The meshes of the sheet used in simulation.

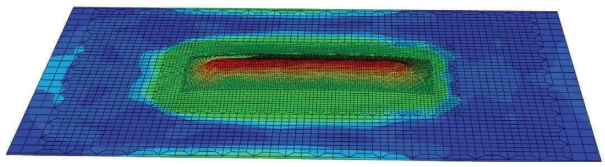

Figure 6: Deformed straight grooves obtained from FE simulation.

Table 1: Average values of forming forces.

	With UV	Without UV
F_x (N)	31.3	33.2
F_z (N)	860.3	866.3
F (N)	860.9	866.9

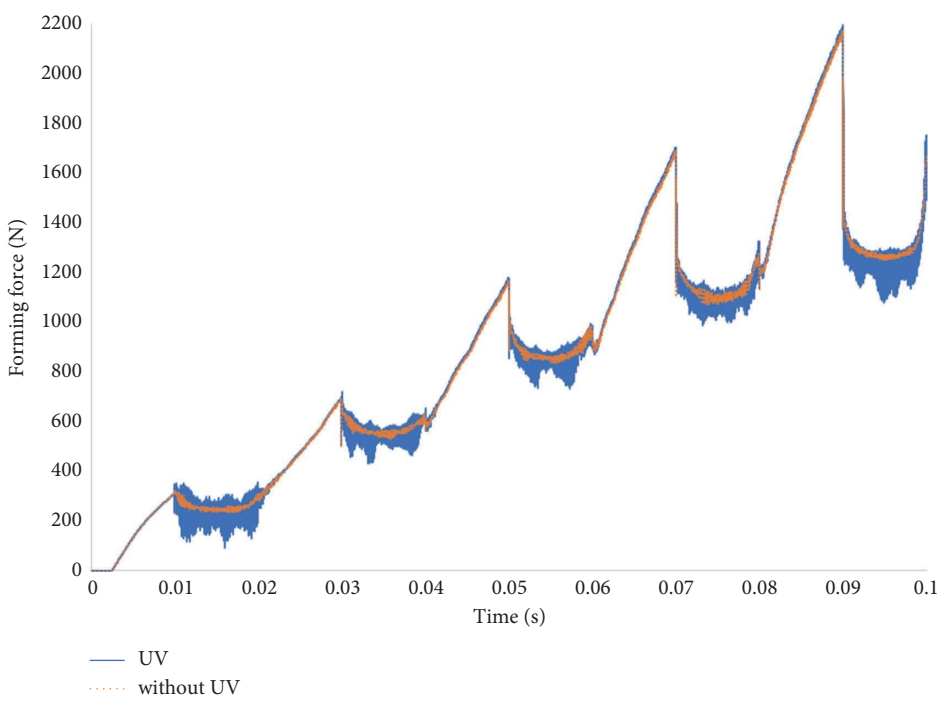

Figure 7: Axial force of straight groove simulation.

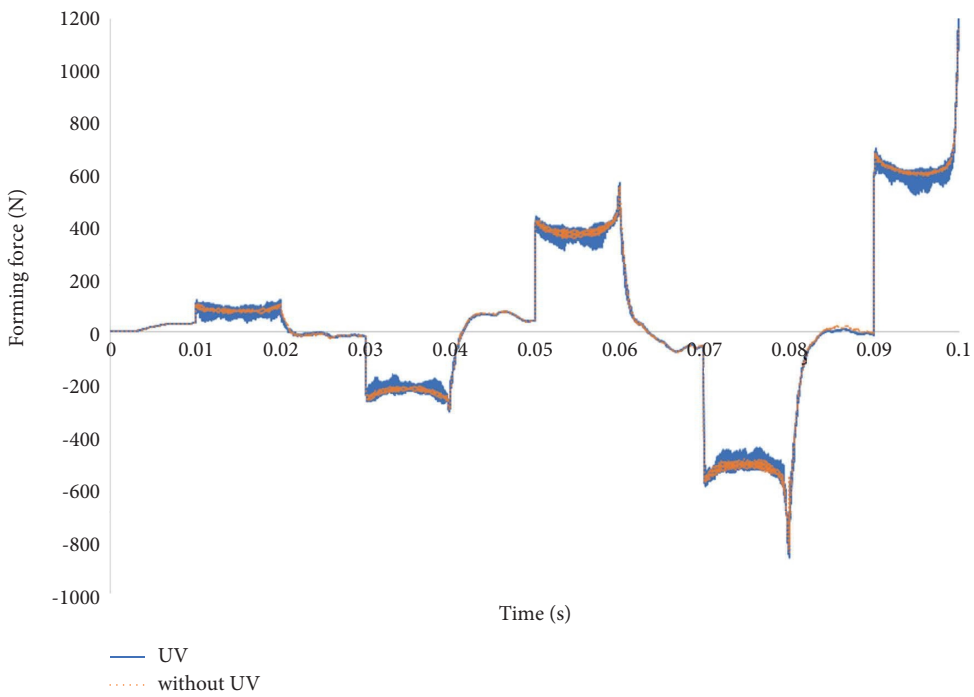

Figure 8: Planar force of straight groove simulation.

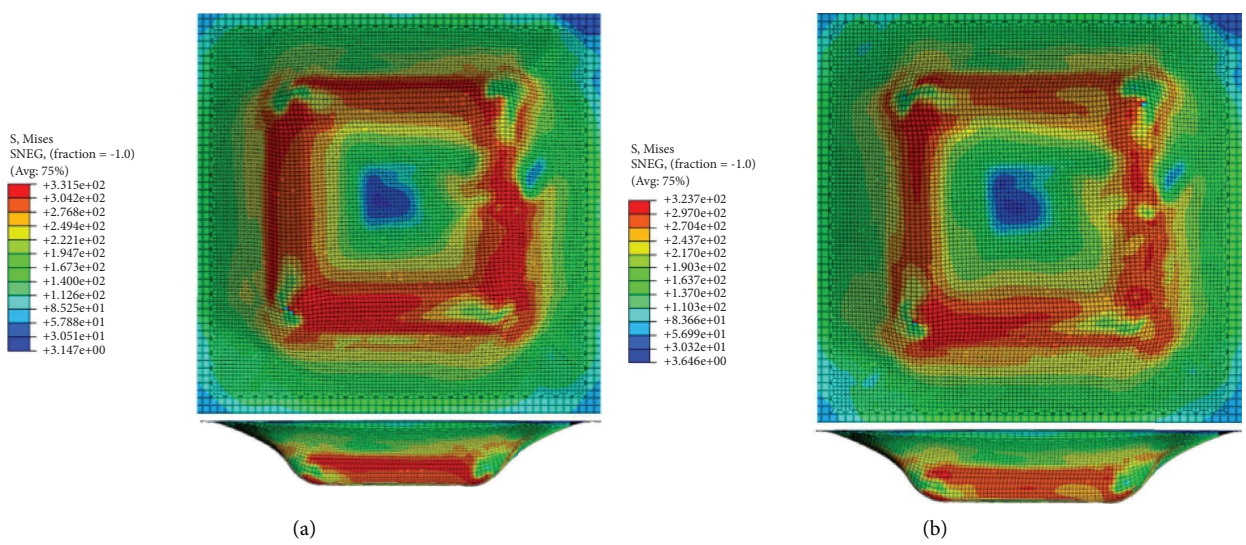

Figure 9: Simulation results of stress: (a) with UV; (b) without UV.

3.3. Simulation of Straight Grooves with Different Parameters. From Figure 11 and Table 3, an increase in the tool diameter led to an increase in forming forces without UV. In UV simulations, the forming force decreases and the change is relatively small (from 0.1 N to 2 N). A large tool means a bigger contact area which led to a bigger deformed area; therefore, it requires more force for forming.

Forming force values, in Figure 12 and Table 4, decrease with UV (average 18.7 N reduction). In reality, a faster rotating tool causes the tool to slide on the sheet surface more, which led to generate heat. High heat will soften up the material that makes tough material easier to be deformed. Besides, heat generated during the process can improve formability.

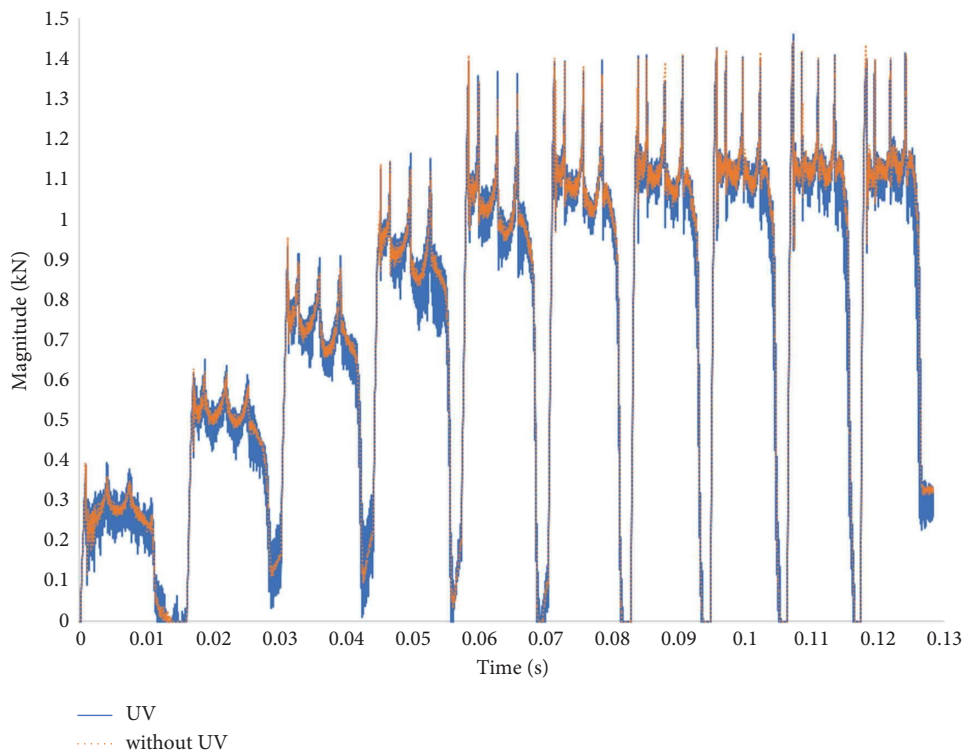

Figure 10: Forming force in the simulation of the truncated pyramid with and without UV.

Table 2: Average forming forces in the simulation of the truncated pyramid.

	With UV	Without UV
F_x (N)	30.6	32.2
F_y (N)	−31.8	−32.0
F_z (N)	751.5	764.7
F (N)	752.8	766.1

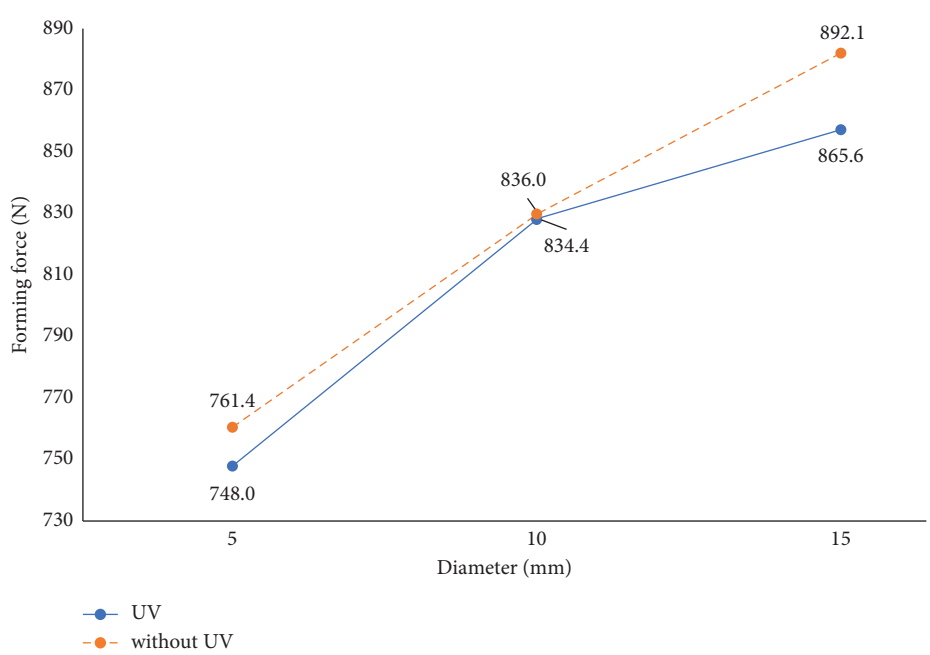

Figure 11: Forming forces with different tool diameters.

Table 3: Simulation setup and results with different tool diameters.

No.	Tool diameter (mm)	Step size (mm)	Amplitude (μm)	Rotational speed (RPM)	Forming force (N)
1	5	1.0	15	0	748.0
2	5	1.0	0	0	761.4
3	10	1.0	15	0	834.4
4	10	1.0	0	0	836.0
5	15	1.0	15	0	865.6
6	15	1.0	0	0	892.1

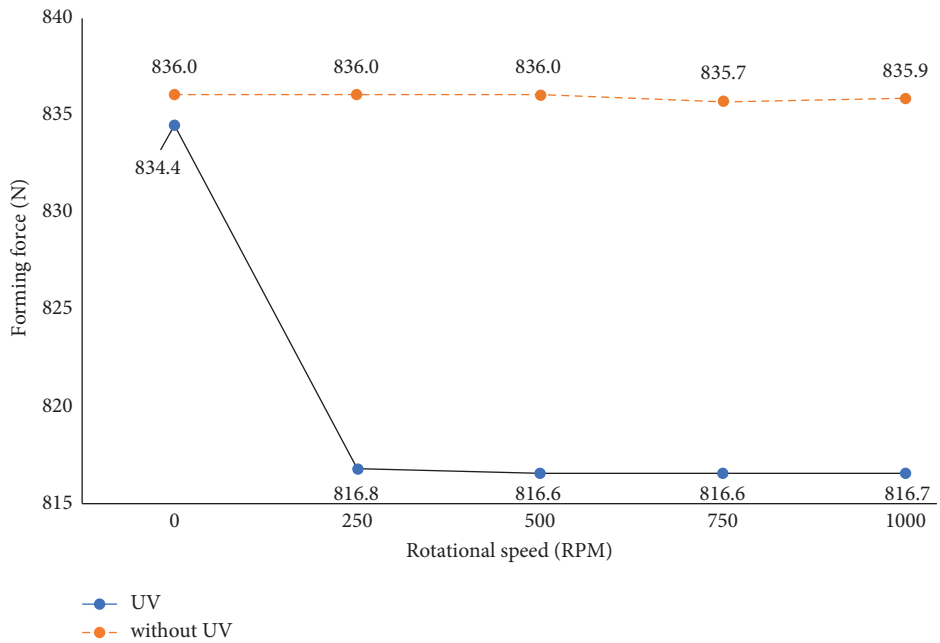

Figure 12: Forming force with different rotational speeds.

Table 4: Simulation setup and results with different rotational speeds.

No.	Tool diameter (mm)	Rotational speed (RPM)	Step size (mm)	Amplitude (μm)	Forming force (N)
1	10	0	1.0	15	834.4
2	10	0	1.0	0	836.0
3	10	250	1.0	15	816.8
4	10	250	1.0	0	836.0
5	10	500	1.0	15	816.6
6	10	500	1.0	0	836.0
7	10	750	1.0	15	816.6
8	10	750	1.0	0	835.7
9	10	1000	1.0	15	816.7
10	10	1000	1.0	0	835.9

Figure 13 and Table 5 show the average values of forming forces with and without UV simulations. The forming force values with different step sizes are higher than other simulations because of the higher forming depth. By changing the step size, forming forces can be greatly increased with the average changing value at 81.2 N

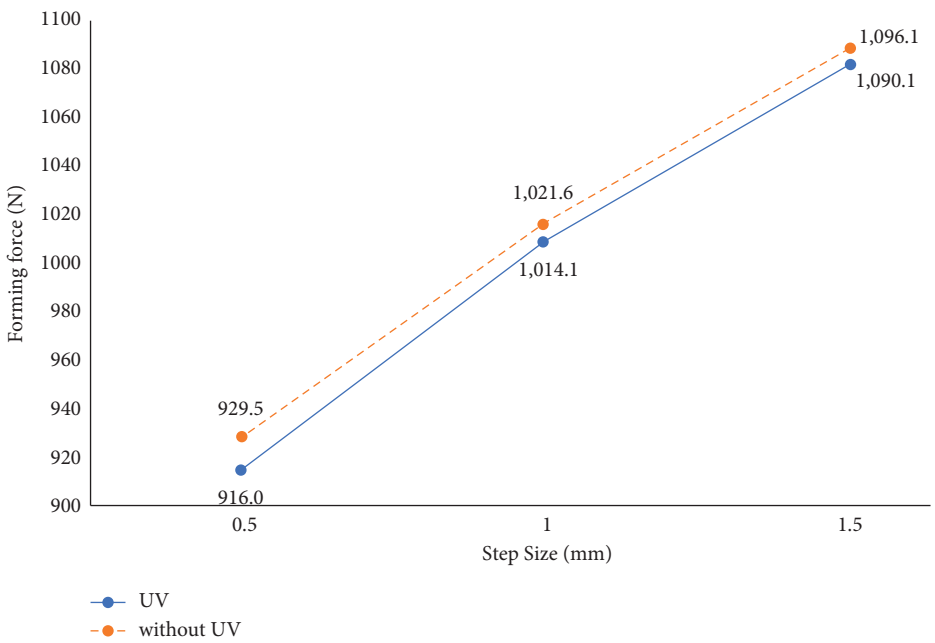

Figure 13: Forming force with different step sizes.

Table 5: Simulation setup and results with different step sizes.

No.	Tool diameter (mm)	Number of step	Part depth (mm)	Step size (mm)	Amplitude (μm)	Forming force (N)
1	10	24	6	0.5	15	916.0
2	10	24	6	0.5	0	929.5
3	10	12	6	1.0	15	1014.1
4	10	12	6	1.0	0	1021.6
5	10	8	6	1.5	15	1090.1
6	10	8	6	1.5	0	1096.1

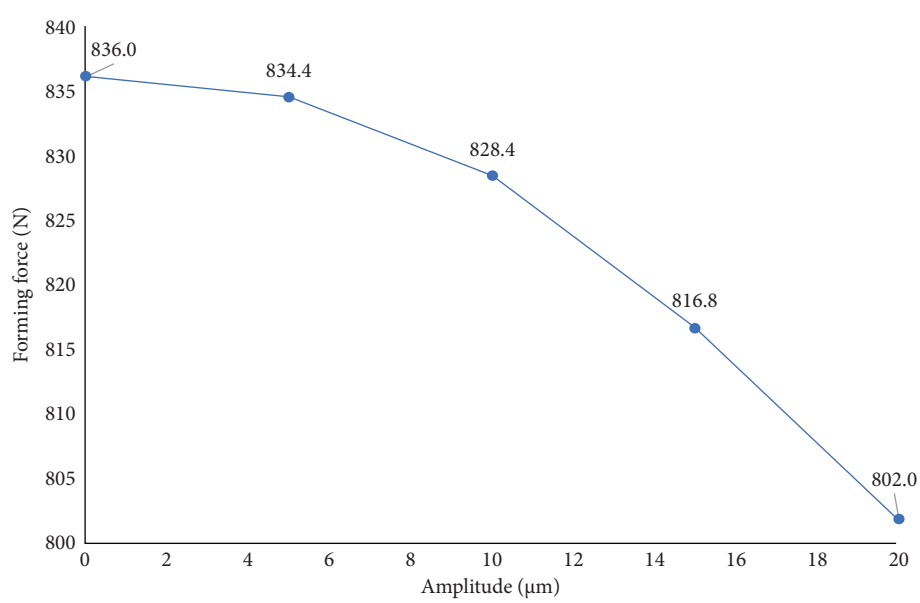

Figure 14: Forming force with different vibrating amplitudes.

Table 6: Simulation setup and results with different amplitudes.

No.	Tool diameter (mm)	Step size (mm)	Amplitude (μm)	Rotational speed (RPM)	Forming force (N)
1	10	1.0	0	0	836.0
2	10	1.0	5	0	834.4
3	10	1.0	10	0	828.4
4	10	1.0	15	0	816.8
5	10	1.0	20	0	802.0

significantly higher than simulations with other parameters. The average value of force reduction between simulations with and without UV is at 16.3 N. Large step size can increase the force needed for deformation due to more materials being deformed.

Furthermore, from Figure 14 and Table 6, high vibrating amplitudes reduce the forming force which is being reported in many articles used in this study.

4. Conclusions

This work presents the design and analysis of the simulation of the vibrating tool in the SPIF process. To observe the force reduction in SPIF with and without ultrasonic vibration, straight groove and truncated pyramid tests were conducted on aluminum alloy 5052. The following conclusions can be made:

(i) Forming forces in conventional SPIF can be reduced by using vibrating tools. These forces fluctuate heavily under the influence of UV due to cyclic contact between the tool and the workpiece. Furthermore, as the depth increases, forming forces also rise and maintain stable values after reaching certain depth.

(ii) Different parameters have different impacts on formability with and without UV. An increase in the rotational tool speed and vibrating amplitude decreases forming forces. In contrast, large step size leads to higher forming forces and lower formability. Tool diameters have limited effects on forming forces.

Data Availability

The data that support the findings of this study are available on request from the corresponding author.

Conflicts of Interest

The authors declare that they have no conflicts of interest.

Authors' Contributions

Trung-Kien Le and Thanh-Hai Nguyen were responsible for methodology, conceptualization, writing the original draft, project administration, and analyzing the experimental data. Duc-Toan Tran was responsible for design and manufacturing a complete test system. Ngoc-Tam Bui was responsible for writing, reviewing, and editing the manuscript and funding acquisition. All the authors have read and agreed to the published version of the manuscript.

Acknowledgments

This work was supported by the Centennial SIT Action for the 100th anniversary of the Shibaura Institute of Technology to enter the top ten Asian Institute of Technology. The authors acknowledge the Ho Chi Minh City University of Technology (HCMUT), VNU HCM, for supporting this study.

References

[1] J. Pujana, A. Rivero, A. Celaya, and L. López de Lacalle, "Analysis of ultrasonic-assisted drilling of Ti6Al4V," *International Journal of Machine Tools and Manufacture*, vol. 49, no. 6, pp. 500–508, 2009.

[2] M. Lotfi, S. Amini, and J. Akbari, "Surface integrity and microstructure changes in 3D elliptical ultrasonic assisted turning of Ti–6Al–4V: FEM and experimental examination," *Tribology International*, vol. 151, Article ID 106492, 2020.

[3] X. Liu, D. Wu, J. Zhang, X. Hu, and P. Cui, "Analysis of surface texturing in radial ultrasonic vibration-assisted turning," *Journal of Materials Processing Technology*, vol. 267, pp. 186–195, 2019.

[4] N. A. Narkevich, E. Deryugin, O. Perevalova, and I. Vlasov, "Effect of ultrasonic forging strain processing on the surface layer microstructure and temperature-dependent mechanical properties of high nitrogen austenitic steel," *Materials Science and Engineering: A*, vol. 834, Article ID 142590, 2022.

[5] Q. Li, Y. Zhang, J. Chen et al., "Effect of ultrasonic micro-forging treatment on microstructure and mechanical properties of GH3039 superalloy processed by directed energy deposition," *Journal of Materials Science & Technology*, vol. 70, pp. 185–196, 2021.

[6] Z. Yin and M. Yang, "Investigation on deformation behavior in the surface of metal foil with ultrasonic vibration-assisted micro-forging," *Materials*, vol. 15, p. 1907, 2022.

[7] S. Patil, "Modelling and simulation of effect of ultrasonic vibrations on machining of Ti6Al4V," *Ultrasonics*, vol. 54, pp. 694–705, 2014.

[8] M. Zhou, "Vibration-assisted precision machining of steel with PCD tools," *Materials and Manufacturing Processes*, vol. 18, no. 5, pp. 825–834, 2003.

[9] T. Tawakoli and B. Azarhoushang, "Influence of ultrasonic vibrations on dry grinding of soft steel," *International Journal of Machine Tools and Manufacture*, vol. 48, no. 14, pp. 1585–1591, 2008.

[10] J. Hung and M. Chiang, "The influence of Ultrasonic-vibration on double backward-extrusion of aluminum alloy," in *Proceedings of the World Congress on Engineering*, London, UK, July 2009.

[11] X. Zhan, Z. Wang, M. Li, Q. Hu, and J. Chen, "Investigations on failure-to-fracture mechanism and prediction of forming limit for aluminum alloy incremental forming process," *Journal of Materials Processing Technology*, vol. 282, Article ID 116687, 2020.

[12] S. Martin, "Rapid prototyping by single point incremental forming of sheet metal," https://backend.orbit.dtu.dk/ws/portalfiles/portal/5061436/SPIF_PhD_Skjoedt.pdf Doctoral Dissertation, Technical University of Denmark, Kongens Lyngby, Denmark, 2008, https://backend.orbit.dtu.dk/ws/portalfiles/portal/5061436/SPIF_PhD_Skjoedt.pdf Doctoral Dissertation.

[13] João Luís Padrão de Brito Câmara, "Single point incremental forming," Master Ddissertation, Universidade Técnica de Lisboa, Lisbon, Portugal, 2009.

[14] K. E. Ali, "Finite element prediction of deformation mechanics in incremental forming processes," https://etheses.bham.ac.uk/id/eprint/1726/ Doctoral Dissertation, University of Birmingham, Birmingham, UK, 2011, https://etheses.bham.ac.uk/id/eprint/1726/ Doctoral Dissertation.

[15] D. S. Malwad and V. M. Nandedkar, "Deformation mechanism analysis of single point incremental sheet metal forming," *Pro-cedia Materials Science*, vol. 6, no. 2211-8128, pp. 1505–1510, 2014.

[16] D. W. Adams, "Improvements on single point incremental forming through electrically assissted forming, contact area pre-diction and tool development," Dotocral Dissertation, Queen's University, Kingston, Canada, 2013.

[17] B. Langenecker, "Effects of ultrasound on deformation characteristics of metals," *IEEE transactions on sonics and ultrasonics*, vol. 13, no. 1, 1966.

[18] H. Sedaghat, "Ultrasonic vibration-assisted incremental forming," Doctoral Dissertation, The University of New South Wales Sydney Australia, Kensington, Australia, 2018.

[19] Y. Li, X. Chen, J. Sun, J. Li, and G. Zhao, "Effects of ultrasonic vibration on deformation mechanism of incremental point-forming process," *Procedia Engineering*, vol. 207, pp. 777–782, 2017.

[20] Y. Long, Y. Li, J. Sun, I. Ille, J. Li, and J. Twiefel, "Effects of process parameters on force reduction and temperature variation during ultrasonic assisted incremental sheet forming process," *International Journal of Advanced Manufacturing Technology*, vol. 97, no. 1-4, pp. 13–24, 2018.

[21] Y. Li, W. Zhai, Z. Wang et al., "Investigation on the material flow and deformation behavior during ultrasonic-assisted incremental forming of straight grooves," *Journal of Materials Research and Technology*, vol. 9, no. 1, pp. 433–454, 2020.

[22] M. Vahdati, R. Mahdavinejad, and S. Amini, "Investigation of the ultrasonic vibration effect in incremental sheet metal forming process," *Proceedings of the Institution of Mechanical Engineers - Part B: Journal of Engineering Manufacture*, vol. 231, no. 6, pp. 971–982, 2017.

[23] R. Cheng, N. Wiley, M. Short, X. Liu, and A. Taub, "Applying ultrasonic vibration during single-point and two-point incremental sheet forming," *Procedia Manufacturing*, vol. 34, pp. 186–192, 2019.

[24] S. Amini, F. Nazari, M. Baraheni, and A. H. Ghasemi, "Investigating the effect of rotation speed and ultrasonic vibrations in the incremental forming process," *Advance Design and Manufacturing Technology*, vol. 11, no. 4, pp. 91–97, 2018, http://admt.iaumajlesi.ac.ir/article_668322.html.

[25] M. Yang, L. Bai, Y. Li, and Q. Yuan, "Influences of vibration parameters on formability of 1060 aluminum sheet processed by ultrasonic vibration-assisted single point incremental forming," *Advances in Materials Science and Engineering*, vol. 2019, Article ID 8405438, 12 pages, 2019.

[26] B. Lang, Y. Li, M. Yang, Y. Lin, Q. Yuan, and R. Zhao, "Modeling and Analysis of Single Point Incre-Mental Forming Force with Static Pressure Support and Ultrasonic Vibration," *Materials (Basel)*, vol. 12, 2019.

[27] R. Slater, "A review of analytical and experimental investigations of the spinforging of sheet metal cones," *Proceedings of the 1st International Conference on Rotary Metal-Working Processes*, Springer, Berlin, Germany, 1979.

[28] B. Cheng, H. Leung, and A. Ngan, "Strength of metals under vibrations– dislocation-density-function dynamics simulations," *Philosophical Magazine*, vol. 95, no. 16-18, pp. 1845–1865, 2015.

[29] X. Xiao, J. J. Kim, M. P. Hong, S. Yang, and Y. S. Kim, "RSM and BPNN modeling in incremental sheet forming process for AA5052 sheet: multi-objective optimization using genetic algorithm," *Metals*, vol. 10, no. 8, p. 1003, 2020.